Anaerobic degradation of acid red 73 by obligately aerobic *Aspergillus tabacinus* LZ-M though a self-redox mechanism

Xuan Yu[1], Simin Zong[1], Chunlan Mao[1*], Aman Khan[1], Wenxue Wang[1], Hui Yun[1], Peng Zhang[2], Xiangkai Li[1*]

1. Ministry of Education Key Laboratory of Cell Activities and Stress Adaptations, School of Life Sciences, Lanzhou University, Tianshui South Road #222, Lanzhou 730000, Gansu, China

2. Key Laboratory for Resources Utilization Technology of Unconventional Water of Gansu province, Gansu Academy of Membrane Science and Technology, Duanjiatanlu #1272, Lanzhou 730020, Gansu, China

***Corresponding Author**

E-mail address: xkli@lzu.edu.cn (Prof. Li); maocl@lzu.edu.cn (Prof. Mao)

Tel: 86-931-8912561

Fax: 86-931-8912560

Abstract

Fungi are potential biological resources for refractory organics degradation, but their anaerobic degradation of azo dyes are rarely reported. In this study, a fungus *Aspergillus tabacinus* LZ-M was isolated grown aerobically and degraded acid red 73 (AR73) with a decolorization rate of 90.28% in 5 days at 400 mg/L of concentration anaerobically. Metabolic pathway showed that AR73 was reduced into 2-hydroxynaphthalene and aniline then mineralized into CO_2. The anaerobic self-redox process revealed electrons generated in carbon oxidation and transferred to -C-N= and -N=N, resulting in complete mineralization of AR73 in strain LZ-M. Data of transcriptome analysis showed that the benzene compounds produced from AR73 by declorizing reductase entered the catechol pathway and glycolysis process to mineralize. Enzymes involved in aromatics degradation, glycolysis processes, cytochrome C and quinone oxidoreductases were up-regulate, but the key reductase responsible to cleave AR73 to phenylhydrazine was not found. A novel enzyme Ord95 containing a glutamate S-transferase domain was identified in the unknown genes as a reductase which cleaving -C-N= in AR73 using NADH as electron donor, and three arginines key active sites. These observations reveal a new degradation mechanism of AR73 in strain LZ-M which would be potential candidate for treatment of azo dyes wastewater.

Keywords: *Aspergillus*; Azo dyes; Transcriptome; Anaerobic decolorization.

Graphical abstract

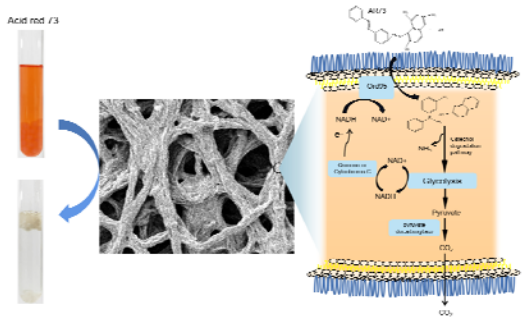

1. Introduction

Azo dyes are widely used as colorants in different fields of its properties, such as vivid colors, tinctorial strength, and ease of manufacturing, and approximately 450 000 tons of azo dyes are consumed annually (*1, 2*). Among 15% of dyes used in the industries are discharged into wastewater (*3*). Dyes are refractory, toxic and mutagenic, inevitably causing extensive pollution in both aquatic and terrestrial systems (*4*). In recent decades, biotechnologies have shown efficiency and affordability advantages in treatment of wastewater containing toxic and refractory dyes (*5*). Especially, bacteria-mediated treatments have emerged to eliminate azo dyes from wastewater (*6, 7*). Nevertheless, the bacterial treatment can only decolorize, but not able to achieve the complete mineralization of azo dyes (*3, 8*). The symmetrically breakdown of azo bond by bacteria is easily to accumulate aromatic amines, which are toxic to organisms and are stubborn for biodegradation (*9*). The asymmetric breakage of azo bond or complete mineralization of azo dyes by microorganisms are rare. Therefore, it is essential to find the microorganisms that can degrade the azo dyes to non-toxic substances.

Fungi, as a decomposer showed significant capabilities in the degradation of toxic and refractory organics including lignin, cellulose, pharmaceuticals, polycyclic aromatic hydrocarbons, and etc. (*10, 11*). Fungi secret non-specific oxidases and completely mineralize these pollutants into CO_2 (*12*). For example, benzo[a]pyrene is mineralized to CO_2 by the white rot fungus *Pleurotus ostreatus* (*13*). *Aspergillus versicolor* LH1 completely degrade methyl red at 200 mg/L of concentration (*2*), and

65 *A. niger* decolorize acid blue 161 up to 58% (*3*). However, the decolorization of azo
66 dyes are commonly more effective under anaerobic than aerobic conditions (*9*). This
67 is because of the azo reduction enzyme for the initial cleavage of the azo bond
68 sensitive to oxygen (*2, 14*). Similarly, the electron withdrawing nature of the azo bond
69 impedes the susceptibility of dye molecules to oxidative reaction and, thus, azo dyes
70 show resistance to aerobic biodegradation (*14*). Fungi commonly grow under aerobic
71 condition, and degradation of azo dyes under anaerobic condition was less reported.

72 Some reports suggest that aerobic microorganisms have potential for anaerobic
73 reaction (*15*). For example, Lysinibacillus sp. NP05 was capable of degrading
74 polychlorinated biphenyls under anaerobic condition (*15*). Pseudomonas denitrificans
75 G1 grew under the aerobic condition, and could achieve effective denitrification under
76 the anaerobic conditions (*16*). An obligately aerobic bacterium, Zetaproteobacteria,
77 has an anaerobic metabolic pathway by genome analysis (*17*). This indicates that
78 enzymes associated with anaerobic function are secreted by this aerobic
79 microorganism. There are evidences that auxiliary anaerobic metabolism exists in
80 obligately aerobic fungi (*18*). An obligately aerobic fungus, A. nidulans, could survive
81 under anaerobic conditions and exists the alcoholic fermentation pathway (*18, 19*). So,
82 fungi have the potential to degrade azo dyes under anaerobic conditions.

83 The bio-degradation process of organic matter is usually accompanied with
84 oxidation and reduction reactions. For example, lignin, plastic and dyes are
85 oxidatively depolymerized by peroxidase (*20*). Anaerobic denitrification of organic
86 nitrogen is a reduction process (*21*). Some organic matters are degraded

87 synchronously by oxidation and reduction in a self-redox process. For instance,
88 bioconversion of organic matter to methane/H_2 during anaerobic biological
89 fermentation (*22*). In a fermentation process, electrons were generated during butyrate
90 oxidation and transferred to H^+ to generate acetate and H_2 (*23*). In this study, a fungus
91 identified as *Aspergillus tabacinus* LZ-M could grow aerobically and degrade acid red
92 73 (AR73) anaerobically. The analysis of metabolic pathway illustrated that LZ-M
93 had a strong ability to mineralize AR73 via self-redox. A novel decolorizing reductase
94 was excavated and its degrading mechanism was revealed. This study provides a new
95 microbial resource for the biodegradation of azo dyes.
96
97 **2. Materials and methods**
98 2.1 Strain isolation and culture
99 To isolate microorganisms adapted to low-nutrient wastewater, a piece of
100 parafilm (PM996) (1 cm × 1 cm) was floated in 100 mL of carbon-free liquid medium
101 (1 g/L NaCl, 1 g/L K_2HPO_4, 1 g/L KH_2PO_4) and inoculated with 1 mL soil sample
102 that was collected in the arboretum of Gansu Academy of Membrane Science and
103 Technology in Gansu Province, China. After stationary culture for 30 days at room
104 temperature (25-28 ℃), flocculent microorganisms were growing around the parafilm.
105 The flocculent microorganisms were transferred into the solid medium of Potato
106 Dextrose Broth Medium (PDB, Solarbio, China), culture for 3 days at 30 ℃. Pick
107 spores into the solid medium of PDB for culturing until pure colonies were formed.
108 For spore collection, using 10 mL 25% glycerol solution to elute the spores on the

surface of the colonies in a solid culture plate, and sucking the spore liquid into the cryogenic tubes and stored it at -80 ℃.

The aerobic growth of this strain was conducted in 250-mL conical flasks containing 150 mL of liquid PDB medium with inoculating 150 uL of spore suspension, and mycelia pellets were formed after culturing for 2.5 days at 30 ℃ and 200 rpm. The spore concentration is about 10^4 /mL, calculated as the number of mycelia pellets formed by liquid culture using serial dilution. For activated culture, the amount of spore inoculum is 1‰.

2.2 Chemicals

Acid red 73 was purchased from Sigma-Aldrich (St. Louis, USA). Methanol and ethyl acetate were HPLC grade. Other reagents were purchased from Solarbio Science & Technology Co.,Ltd. Beijing, China.

2.3 Anaerobic decolorization of fungi

Mycelia pellets from 300 mL aerobic activated medium were collected by filtration and washed for 5 times using ddH_2O and then used for anaerobic degradation experiment. One liter of basal mediun (BM) contained 1 g/L NaCl, 1 g/L KH_2PO4, 1 g/L K_2HPO_4, and pH 7 was used to suspend the mycelium pellets. To analyze the ability of fungi to decolorize AR73 under anaerobic condition, AR73 solutions were added into the medium to arrive the concentration of 50 mg/L. The 100 mL of the mixed mycelium suspension was added to 250 mL anaerobic flasks respectively. Anaerobic flasks was filled with nitrogen for 20 min and stationary incubated in an anaerobic incubator at 30 ℃ (n=3). For anoxic culture, anaerobic

flasks without nitrogen pouring were incubated at 30 ℃ in static phase. For aerobic culture, flasks were rotationally incubated at 30 ℃ and 200 rpm. Experiment used sterile medium as controls. The samples were taken at different time interval for analysis.

2.4 Effect of operation parameters on biodecolorization

The biodecolorization performance of AR73 by strain LZ-4 was evaluated under different culture conditions. Mycelia pellets from 900 mL aerobic activated medium were suspended in 3 L BM and divided into anaerobic bottles with 100 mL per bottle. To examine the effect of additional carbon sources, 1 g/L of soluble starch, glucose, potato, tyrptone, PDB medium were added into BM containing 50 mg/L AR73, respectively. To examine the effect of pH, the initial pH was adjusted to 3, 4, 5, 6, 7, 8, 9, 10, and 10.5. In AR73 load experiments, the initial AR73 concentrations ranged from approximately 50-500 mg/L. To evaluate the ability of the strain LZ-M for other dyes and refractory organics removal, 50 mg/L methyl orange, 50 mg/L neutral red, 30 mg/L malachite green, 10 mg/L metronidazole, 30 mg/L furazolidone and 30 mg/L 3,5-dinitrosalicylic acid were added into BM, respectively. In order to test the long-term anaerobic decolorization by strain LZ-M, 2.5 mL of 2g/L AR73 was added to the anaerobic bottle when the color of the dye in the culture solution was disappeared, continuously, until occurring incomplete depigmentation after 24 hours. Unless the single-factor was adjusted as per the experimental design, the initial concentration of AR73 concentration was 50 mg/L. The fungal suspension was incubated for 5 days at 30 ℃ under anaerobic condition, and samples were collected

153 to determine the concentrations of substrate. All experiments were performed in three
154 duplicate.

155 2.5 LC/MS analyses of metabolites

156 After anaerobic degradation of 50 mg/L AR73 by strain LZ-M for 3 days, the
157 culture supernatant was collected and sent to Wuhan Metware Biotechnology Co.,Ltd.
158 for LC/MS analysis. Metabolic identification information was obtained by searching
159 the company's database.

160 2.6 Analysis of ITS sequencing and transcriptome sequencing

161 Mycelia pellets of strain LZ-M after aerobic growth were collected and send to
162 Shanghai Majorbio Bio-pharm Technology Co.,Ltd (Shanghai, China) for DNA
163 extraction and ITS sequencing.

164 To prepare the sample for transcriptome analysis, mycelia pellets of *A. tabacinus*
165 LZ-M after aerobic growth were transferred to BM containing 50 mg/L AR73, filled
166 with nitrogen for 20 min and cultured for 3.5 hours under anaerobic condition at
167 30 ℃. The culture cells were cultured at 200 rpm under aerobic condition were used
168 as a control. After that, mycelia pellets were collected and send to Shanghai Majorbio
169 Bio-pharm Technology Co.,Ltd (Shanghai, China) for RNA extraction and
170 transcriptome sequencing.

171 2.7 Cloning of unknown genes

172 The genes sequence of Ord95 and Ord118 was represented in supplementary and
173 were clone as follows; the Ord95 fragment was amplified from the transcriptome
174 RNA by polymerase chain reaction (PCR) using the primers Ord95F:

175 5'-CCGGAATTCATGTCAGATTCCACGCTCTACC-3' and Ord95R:
176 5'-CCGCTCGAGGCCCTCCAACGCATCTTC-3'. The Ord118 fragment was PCR
177 using the primers Ord118F: 5'-CCGGAATTCATGGCTACTCAAGCTATTCAC-3'
178 and Ord118R: 5'-CCCAAGCTTGCGGTGATGCAGCATGTC-3'. The Ord95 and
179 Ord118 fragments were digested with restriction endonucleases and inserted into
180 plasmid pET-28a, respectively. The recombinant plasmids pET28/Ord95 and
181 pET28/Ord118 were transformed into *E.coli* Rosseta (DE3). For protein-induced
182 expression, the cells were grown in Luria-Bertani medium containing Kanamycin (50
183 μg/mL) and Chloramphenicol (30 μg/mL) at 37 ℃. When cells grown to an OD_{600} of
184 0.6, 0.2 mM isopropyl β-D-1-thiogalactopyranoside was added to the medium and
185 was then cultured for 20 h at 16 ℃. Purification of protein followed as a previous
186 study (*24*). The purified protein was detected using SDS-PAGE, and protein
187 concentration was detected using Pierce BCA Protein Assay Kit (Thermo Fisher
188 Scientific, United States).

189 Various Ord95 mutants were constructed by Phusion™ Site-Directed
190 Mutagenesis Kit (Thermo Fisher Scientific, United States). The procedures for the
191 expression and purification of these variants were similar to that of wild type Ord95.

192 2.8 Enzyme assay of Ord118, Ord95 and its mutants

193 To explore NADH dehydrogenase activity of purified Ord118 and Ord95, the
194 enzyme assay was performed in 3 mL 20 mM Tris-HCl buffer (pH 7.0), containing
195 0.28 mg/L protein, 200 μM NADH and was kept at 37 ℃ for 120 min. The reaction
196 solution was placed in a cuvette, and the absorbance change of NADH was detected

by UV-Spectrophotometry (Hitachi U-3900H) at 340 nm in real time. To explore the AR73 declorizing activity of purified proteins, the enzyme assay was performed in 5 mL of 20 mM Tris-HCl buffer (pH 7.0) containing 0.28 mg/L protein, 25 mg/L AR73 and 200 uM NADH. The reaction solution was injected into vacuum tubes in an anaerobic incubator and kept at 37 ℃ for 48 h, and 200 uL reaction solution was taken out from the vacuum tube every 12 h to measure the absorbance of AR73 at 510 nm. Reaction with predenaturation protein treated for 15 min at 95 °C were used as controls.

2.9 Analytical methods

The surface structure of mycelia pellets of *A. tabacinus* LZ-M was observed by scanning electron microscopy (JEOL JSM-IT500LA). Spectrophotometry was used to measure the concentrations of AR73, methyl orange, neutral red and malachite green at wavelength of 510 nm, 462 nm, 523 nm and 620 nm, respectively. Concentrations of metronidazole, furazolidone, and 3, 5-dinitrosalicylic acid were determined using UV-Spectrophotometry (Hitachi U-3900H) at wavelength of 320 nm, 370 nm and 350 nm, respectively.

Phenylhydrazine and aniline in the culture and enzymatic reaction solutions were detected by high-performance liquid chromatography (HPLC, Agilent 1260). HPLC analysis utilized an Agilent Eclipse XDB-C18 (4.6 mm ×250 mm, 5μm), the mobile phase was methanol/H_2O solution (40:60, v/v) at a flow rate of 1.5 mL/min. An injection volume of 10 uL was used and the UV detection was performed at 280 nm. The consent of CO_2 produced in headspace of anaerobic bottle was detected by gas

chromatography (Agilent 6890N). The injector was set at 240 ℃, the amount of gas sample in each injection was 20 uL, and a split less mode (60 mL/min) was used.

2.10 Statistical analysis

Statistical analyses were performed using SPSS v.17 software and Excel 2010. One-way Analysis of Variance was used to assess differences in the abundance of taxa and then values are presented as the mean ± standard error. Subsequently, Tukey's test was used to determine the sample means that were significantly different.

3. Results and discussion

3.1 The identification of anaerobic AR73 degradation fungus

A fungus growing on parafilm surface in liquid medium was isolated which has 100% similarity to *Asperillus tabacinus* NRRL 4791, and named as *Aspergillus tabacinus* LZ-M (Fig. 1A). The isolated strain LZ-M was grow at 150-250 rpm, where the biomass growth rate increased with the rotation speed (Fig. S1), while less than 100 rpm strain LZ-M growth was inhibited. This result indicated that strain LZ-M was obligately aerobic fungus. The mycelium pellets of strain LZ-M was formed after aerobic growth, and placed it in an anaerobic environment. After 24 h, bubbles were generated in the culture medium, carrying the mycelium to the top of liquid (Fig. 1B). Furthermore, the dye AR73 was completely decolorized after 48 hours of incubation in anaerobic condition. Scanning electron microscope images confirmed the softening of hyphae caused by gas secretion (Fig. 1C). This data indicates that the aerobic strain LZ-M uses AR73 as a substrate for respiration and metabolism under anaerobic

241 environment.

242 *Aspergillus* fungi growing under aerobic condition (*2, 25*), which was consistent
243 with *A. tabacinus* LZ-M reported in this study. The mycelium pellets and morphology
244 are also similar to the *Aspergillus* species, such as *A. niger* and *A. versicolor* (*26, 27*).
245 The mycelium of strain LZ-M produced gas and decolorized AR73, surviving in
246 anaerobic environment. Similarly, anaerobic degradation of azo dyes by bacteria were
247 also reported previously. For example, *S. oneidensis* MR-1 showed a decolorization
248 capability for Cationic Red and *Pseudomonas sp*. SUK1 could decolorize dye Red
249 BLI (*6, 28*). This phenomenon suggests that *A. tabacinus* LZ-M can be used as a
250 potential strain for degradation of the azo dyes as similar as bacterial species.

251 3.2 The characteristics of dye degradation by *A. tabacinus* LZ-M

252 The decolorization ability of *A. tabacinus* LZ-M was compared under
253 aerobic and anaerobic conditions (Fig. 2A). The results showed that strain LZ-M
254 completely decolorized (96.8%) of AR73 in 50 mg/L of concentration at 40 h under
255 anaerobic conditions. However, under aerobic conditions, mycelium does not have the
256 ability to decolorize. The effect factors on anaerobic decolorization efficiency were
257 analyzed. The addition of organic carbon sources, including glucose, PDB medium,
258 tryptone, potato and soluble starch can promote strain LZ-M for decolorization.
259 Among them, soluble starch increased the decolorization ratio from 36.21% to 93.8%
260 within 18 h of incubation (Fig. 2B). The different initial concentrations of AR73 were
261 tested (Fig. 2C). Strain LZ-M completely degraded AR73 in 200 mg/L while the
262 removal rates were decreases to 96.33, 90.28 and 58.72 % in the 300, 400, and 500

263 mg/L of concentrations respectively. The anaerobic reaction achieved complete
264 decolorization of 50 mg/L AR73 at a wide pH range of 4-10.5 and the removal rate
265 was decreased to 43.09% in pH 3 (Fig. 2D). In the anaerobic degradation of
266 multi-batch, this strain could completely degrade 50 mg/L AR73 for 5 times, and the
267 decolorization efficiency began to decline at 5th addition (Fig. 2E). Degradation
268 ability test of strain LZ-M on other organic matter under anaerobic condition was
269 shown in Fig. 2F. The results revealed that strain LZ-M degraded 99.98%, 75.87%,
270 42.55%, 50.315%, 87.375% and 57.43%, of 50 mg/L methyl orange, 50 mg/L neutral
271 red, 30 mg/L malachite green, 10 mg/L metronidazole, 30 mg/L furazolidone, and 30
272 mg/L 3,5-dinitrosalicylic acid within 5 days respectively. The content of these
273 organics in aerobic culture was not changed (data not shown).

274 White rot fungus *Schizophyllum* adsorbs Acid Red 18 (100 mg/L) with a
275 decolorization rate of 27% within 120 h (*29*). Another fungi *A. oryzae* showed 72.38%
276 biosorption decolorization of Acid Red 337 (200 mg/L) (*30*). In contrast, this research
277 reported the complete decolorization of 100-200 mg/L AR73 by strain LZ-M,
278 showing a higher decolorization efficiency compared to the absorption of
279 *Schizophyllum* and *A. oryzae*. The decolorization of strain LZ-M was also compared
280 with the bacteria strains. *Stenotrophomonas sp*. BHUSSp X2 can achieve 90%
281 decolorization of 500 mg/L Acid Red 1, while the effective decolorization is limited to
282 pH 7-8 (*31*). *Bacillus thuringiensis* can achieve 60% decolorization of 500 mg/L acid
283 red 119 (*32*). In this study, the strain LZ-M decolorized AR73 of 500 mg/L with a
284 removal rate of 58.72% at 4-10.5 of pH ranges. The capability of stain LZ-M for

decolorizing high concentrations of acid red under anaerobic condition was comparable to that of *Bacillus thuringiensis* (*32*), and the pH range of stain LZ-M for decolorizing was wider than *Stenotrophomonas sp.* BHUSSp X2 (*31*). These results showed the application advantage of *A. tabacinus* LZ-M in the environmental biotechnology, such as decolorizing industrial dyes with high concentrations and changing pH. This continuous multi-batch decolorization experiment demonstrated the potential of strain LZ-M in dye wastewater treatment. And its degradation on a broad of organics indicated that it is a promising candidate in pollutant treatment.

3.3 The degradation pathway of AR73 in *A. tabacinus* LZ-M

In order to analyze the anaerobic degradation pathway of AR73, the degradation products of AR73 by *A. tabacinus* LZ-M were detected by LC-MS. The results showed that 17 compounds were identified in the AR73 degradation (Table S1). Putative degradation pathway of AR73 was shown in Fig. 3A. The first and second step of degradation of AR73 was to produce phenylhydrazine and hydroxynaphthalene by the cleavage of -C-N= bonds through hydrogenation reduction. And then, phenylhydrazine was deaminated to aniline. Hydroxynaphthalene and aniline was hydroxylating and opening the benzene ring to generate carboxylic acid compounds. Carboxylic acid compounds were decarboxylated to produce CO_2. The concentrations of phenylhydrazine and aniline was detected in the culture medium (Fig. 3B and C). With the increase of time, the concentration of aniline kept increasing, while the concentration of phenylhydrazine decreased after 48h, indicating that the intermediate metabolites phenylhydrazine was

307 further denitrogenated into aniline. Gas produced in anaerobic reaction flasks was
308 identified as CO_2 by gas chromatography. The content of CO_2 increased to 19.56%
309 after 72 h in AR73 medium, and it was only 3.5% in the carbon-free control (Fig. 3D).
310 This indicated that AR73 was mineralized into CO_2 by *A. tabacinus* LZ-M under the
311 anaerobic condition.

312 The degradation of AR73 to benzenes were mainly achieved by the cleavage of
313 -C-N= bonds. *A. versicolor* LH1 degrades methyl red by breaking the -C-N= bond
314 linked with benzene (*2*). Degradations of disperse yellow 3 and acid orange 7 by
315 *Phanerochaete chrysosporium* are also achieved by the -C-N= cleavage (*33*). In this
316 study, the -C-N= cleavage by the strain LZ-M is similar to these fungi. In reports
317 about the bacterial strains, the degradation of Acid Red 1 by *Stenotrophomonas sp.*
318 BHUSSp X2 is achieved by -N=N- cleavage (*31*). Azoreductase derived from
319 *Sphingomonas xenophaga* BN6 degrades azo dyes also through -N=N- cleavage (*33*).
320 This indicates that the degradation of azo dyes by strain LZ-M is different from the
321 anaerobic degradation of these bacteria. In a previous study, naphthalene or benzene is
322 hydroxylated and then benzene ring is opening at the hydroxyl position (*34*). This is
323 consistent with the degradation pathway of hydroxynaphthalene and aniline in this
324 study. The mineralization of benzene compounds to generate CO_2 was achieved in
325 white rot fungi and soil microbe (*35, 36*). The produce of CO_2 indicated that the
326 intermediate produces were mineralized to CO_2. In totally, the degradation of AR73 is
327 mainly achieved by deamination and decarboxylation. AR73 was the sole source of
328 carbon and nitrogen, which acted as both an oxidant and a reductant in the reaction, so

329 the degradation was achieved by self-redox process. The similar phenomenon was
330 found in a previous study that *Syntrophomonas wolfei* can degrade butyrate to CO_2
331 and H_2 (*23*). During this self-redox reaction, the oxidant of AR73, and the reductant is
332 the benzene compounds produced by AR73 decomposition.

333 3.4 Transcriptome analysis of fungi under aerobic and anaerobic conditions

334 In order to analyze the anaerobic degradation mechanism of *A. tabacinus* LZ-M,
335 the differences of gene expression between aerobic and anaerobic conditions were
336 analyzed by transcriptome sequencing. Under anaerobic conditions, a total of 4472
337 differentially expressed transcripts were found, including 2156 up-regulated
338 transcripts and 2316 down-regulated transcripts (Fig. S2). The function types of
339 up-regulated transcripts were shown in Table S2, and 1271 transcripts displayed
340 unknown function, accounted for 51.81% of up-regulated transcripts. In addition,
341 carbohydrate transport and metabolism including 167 transcripts was the most varied
342 functional type. This indicated that carbohydrate transport and metabolism were
343 significantly changed under anaerobic condition. Genes related to cytochrome C
344 oxidoreductase, quinone oxidoreductase and the biodegradation of aromatics were
345 significantly up-regulated (Fig. 4). A complete set of genes involved in the glycolysis
346 process was found in the transcriptome and exhibited high expression levels (Fig. 4).
347 The gene expression of pyruvate decarboxylase was up-regulated considerably, and it
348 increased from 11.5 transcripts to 939.8 transcripts per million reads. This indicated
349 that the anaerobic carbon metabolism in strain LZ-M might be achieved by glycolysis
350 and pyruvate decarboxylation.

In the degradation of AR73, the gene expression of enzymes involved in aromatics biodegradation, glycolysis and electron transfer were discovered, while the expression of gene involved in anaerobic decoloriztion or azoreduction was not found. The enzymes of aromatics biodegradation including 3-hydroxybenzoate 4-monooxygenase, 3-hydroxybenzoate 6-hydroxylase, and catechol 1,2-dioxygenase. Catechol 1,2-dioxygenase is able to degrade benzene, toluene and ethylbenzene (*37*). 3-hydroxybenzoate 4-monooxygenase and 3-hydroxybenzoate 6-hydroxylase are involved in benzoate degradation (*38, 39*). They may be involved in the metabolism of aniline and hydroxynaphthalene. Both aniline and naphthalene degradation intermediates salicylic acid, can enter the glycolysis process through glycosylation and phosphorylation for further metabolism (*40, 41*). In the glycolysis process, the splitting of the six-carbon glucose molecule into two pyruvate molecules by anaerobic oxidation (*42*). Pyruvate can be decarboxylated to acetaldehyde and CO_2 by pyruvate decarboxylase in a stage of fungal anaerobic fermentation (*19*). Therefore, the CO_2 generated in the anaerobic culture was considered as the result of anaerobic oxidation by glycolysis and fermentation (Fig. 3D). These results showed that strain LZ-M can completely mineralize AR73 to CO_2 under anaerobic conditions.

During the glycolysis, NADH is produced and it need to regenerate NAD+ by dehydrogenation (*42*). NADH dehydrogenation requires electron transfer to the oxidized substrate, while the alcohol dehydrogenase that reduces acetaldehyde with NADH was rarely expression under anaerobic conditions (Fig. 4). Therefore, the regeneration of NAD+ may be combined with the cleavage of -C-N= bond of AR73.

373 Cytochrome C oxidoreductase and quinone oxidoreductases often act as mediators of
374 electron transfer in cellular activities (*43*). Gene involved in the electron transfer
375 reactions are found to increasing expression during anaerobic organic degradation
376 (*22*). The up-regulation of cytochrome C oxidoreductase and quinone oxidoreductase
377 may assist in electron transferring and electron balance during self-redox degradation
378 of AR73. The self-redox reaction was represented as follow.

379 $$C_{22}H_{14}N_4Na_2O_7S_2 + 16NADH \xrightarrow{\text{Reduction}} C_{10}H_8O + 2C_6H_6 + 4NH_3 \quad \text{(Eq.1)}$$

380 $$C_{10}H_8O + 2C_6H_6 \xrightarrow{\text{Oxidation}} 22CO_2 + 20\,NADH \quad \text{(Eq.2)}$$

381 The degradation of AR73 was mainly achieved through carbon oxidation and
382 nitrogen reduction. During the reduction process, 12 NADH are needed to decompose
383 one molecule of AR73 to produce 4 molecules of NH_3 (Eq.1). Similarly,
384 hydroxynaphthalene and benzene analogs produced by one molecule of AR73 were
385 completely mineralized to produce 22 molecules of CO_2 and 20 NADH in oxidation
386 process (Eq.2). It can be calculated by electron balance that when the self-redox
387 equilibrium occurs, 80% of the carbon can be mineralized and converted into CO_2.
388 Azoreductase from bacteria and lignin peroxidase, manganese peroxidase and laccase
389 from the fungi are able to degrade azo dyes (*33*), while they are not expression in
390 strain LZ-M under anaerobic condition. Genes annotated as unknown function
391 accounted for 51.81% of up-regulated transcripts. Thus, there may be new
392 decolorizing enzyme among unknown genes that worth to explore.

393 3.5 Cloning and expression of unknown genes

394 The up-regulation genes were further screened based on the criteria that

transcript expression level more than 150 counts and expression up-regulated fold more than 4.0, and then 140 genes was obtained. Among them, 51 genes were classified as oxidoreductase in enzymatic classification, 60 genes belonged to other classifications, and 29 genes belonged to unknown genes (Fig. 5A). Based on expression similarity (*44*), unknown genes have a high probability of being redox genes. Two unknown genes, named ord95 and ord118, have been cloned into *E.coli* Rosetta (DE3) and expressed by induction. The two proteins were purified successfully and detected by SDS-PAGE method (Fig. 5B). Alignment in NCBI database, the Ord95 gene showed the highest sequence identity of 58.71% with aconitate hydratase from *A. tubingensis*. Ord118 showed 100% similarity to hypothetical protein and no similarity to other functional proteins. The NADH dehydrogenase activity assay showed that both of them had NADH dehydrogenase activity (Fig. 5C and D). When the concentration of protein was 0.28 mg/L, the absorbance of NADH at A340 nm reduced at rate of 0.001 /min and 0.00043 /min by Ord118 and Ord95, respectively. Protein Ord95 and Ord118 were also found to have NADH-DCIP reductase activity using Biyuntian NADH oxidase detection kit (Fig. S3). These results suggest that both Ord95 and Ord118 are redox type enzymes. The enzyme activity analysis of AR73 decolorization using NADH as electron donor was conducted, and Ord95 had anaerobic decolorization enzyme activity (Fig. 5E and F), and the optimal reaction conditions of the enzymatic anaerobic decolorization were 37℃ and pH 7.0 (Fig. S4). It couldn't decolorize under aerobic conditions. When the concentration of AR73 was 25 mg/L and the concentration of Ord95 protein was 0.28

417 mg/L, the decolorization rate of AR73 was 0.4696 mg/L/h. This result confirms that
418 Ord95 is a decolorizing reductase, and it might be the enzyme involved in the
419 anaerobic decolorizing of AR73.

420 3.6 Analysis of the decolorization mechanism of protein Ord95

421 In the degradation of AR73 by Ord95, aniline and phenylhydrazine were detected
422 by HPLC in enzymatic reaction (Fig. 6A). The content of phenylhydrazine was
423 increased at 24 h and decreased at 48 h, while the content of aniline kept increasing
424 (Fig. 6B). This suggestion that Ord95 is the enzyme that broke the AR73 of -C-N=
425 bond and its products were similar to fungal. Alignment in NCBI database, the 26-80
426 position of Ord95 sequence is similar to the glutathione S-transferase N-terminal
427 domain with E-value of 7.07e-03, suggesting that this domain may be its active region.
428 The main active site of glutathione transferase usually contains arginine (R) and
429 tyrosine (Y) (*45*). The arginine and tyrosine near the domain region on the Ord95
430 were mutated to alanine (A), including 7Y, 8Y, 38R, 54R, 55R, 67Y. The 6 mutant
431 proteins were expressed and purified (Fig. 6C), and their decolorizing activity was
432 analyzed (Fig. 6D). Compared with Ord95 protein, the enzyme activity of mutants
433 38R>A, 54R>A, 55R>A decreased significantly to 43.1%, 17.43% and 36.9%,
434 respectively. The enzyme activity of mutants 7Y>A, 9Y>A, 67Y>A did not change
435 significantly. It suggested that 38R, 54R, 55R may be the active site of Ord95.
436 Searching for template of 3D structure model of Ord95 in SWISS-MODEL, *C.*
437 *albicans* actin binding protein 6m4c.1.A exhibited the highest quaternary structure
438 quality estimate (QSQE) of 0.26, and the sequence identify was 32.98%. It suggests

that Ord95 is a novel protein and its function has not been analyzed. Thus, 6m4c.1.A was selected as the template for use in homology model constructions of Ord95 by SWISS-MODEL. The functional domain of this protein was simulated as shown in the Fig. 6E and F. The model was a dimer with each monomer consisting of 1 beta sheet and 3 alpha helices.

Three arginines were identified as the key sites of Ord95. The active site of glutathione transferases containing arginine is found in previous study (*45*). Arginine is an amino acid containing a guanidine group, which catalyzes the cycle of ornithine, promotes the formation of urea in organisms and turns ammonia into urea (*46*). Ord95 can aminate AR73 to form phenylhydrazine and aniline, which is associated with nitrogen metabolism. Therefore, the presence of arginine might promote the amination of nitrogen during AR73 degradation by Ord95. The degradation products of AR73 by the enzyme are similar to the degradation products by strain LZ-M, indicating that Ord95 is the functional enzyme for anaerobic decolorization. The metabolic mechanism of AR73 in strain LZ-M was represented in Fig. S5.

Accordingly, it was proved that strain LZ-M had a strong ability to completely mineralize azo dyes under anaerobic conditions, making up for the shortcomings of bacteria. This is the first report of the anaerobic degradation of azo dyes by obligately aerobic fungus. Besides, through the excavation of functional enzymes, new decolorizing enzymes were found, and the degradation mechanism of self-redox was revealed, which has not been reported in previous studies. Under anaerobic conditions, this self-redox degradation is rapid and complete. AR73 act as carbon and nitrogen

source, reduced using NADH as an electronic donor and oxidized in glycolysis by strain LZ-M. Ord95 could cleave -C-N= in AR73 in the first step, and NADH generated during glycolysis can be delivered to Ord95. Fungi possess strong abilities to degrade refractory organic matter and secrete many function enzymes (*47, 48*). There are 128 *Aspergillus* genomes in the NCBI genome database, and 10,000-13,000 proteins were detected in each genome. Therefore, the excavation of fungal functional proteins has great application potential. However, the studies committed to organics degradation mechanism and functional proteins in fungi are still limited, and transcriptome analysis in this study revealed that a large number of proteins in strain LZ-M have not been identified yet. Furthermore, expanding of the protein library of fungi and the excavating functional enzymes might be focused in the further research.

Acknowledgments

This work was supported by National Natural Science Foundation Grant (No: 31870082, 32070117), International Science and technology Cooperation project of Gansu Province (No: 2021-0204-GHC-0019), Gansu Science and Technology Association project (No: GKX20210506-16-5) and Lanzhou science and technology plan project (grant numbers: 2019-4-40). We thanks the Central Lab of School of Life Sciences, Lanzhou University for providing necessary equipment.

Date availability

Transcriptome data of *A. tabacinus* LZ-M under aerobic culture and anaerobic culture is deposited at the Sequence Read Archive (https://www.ncbi.nlm.nih.gov/)

under the accession numbers SRR14455363 and SRR14455360, respectively. The ITS gene sequence of *A. tabacinus* LZ-M is deposited under the accession numbers MZ127527 in NCBI (https://www.ncbi.nlm.nih.gov/search/all/?term=MZ127527). Data of LC-MS metabolite analysis are in the attachments named LC-MS_CK_vs_AR73_neg_info and LC-MS_CK_vs_AR73_pos_info.

Reference

1. P. M. Miladinova, R. K. Vaseva, V. R. Lukanova, On the synthesis and application of some mono-and dis-azo acid dyes. *J. Chem. Technol. Metall* **51**, 249-256 (2016).
2. C. Y. Hu, H. Y. Cheng, X. M. Yao, L. Z. Li, H. W. Liu, W. Q. Guo, L. S. Yan, J. L. Fu, Biodegradation and decolourization of methyl red by Aspergillus versicolor LH1. *Preparative biochemistry & biotechnology* **51**, 642-649 (2021)10.1080/10826068.2020.1848868).
3. E. J. R. Almeida, C. R. Corso, Decolorization and removal of toxicity of textile azo dyes using fungal biomass pelletized. *International Journal of Environmental Science and Technology* **16**, 1319-1328 (2018)10.1007/s13762-018-1728-5).
4. S. Mahmood, A. Khalid, M. Arshad, T. Mahmood, D. E. Crowley, Detoxification of azo dyes by bacterial oxidoreductase enzymes. *Critical reviews in biotechnology* **36**, 639-651 (2016); published online EpubAug (10.3109/07388551.2015.1004518).
5. Y. Huang, X. Hou, S. Liu, J. Ni, Correspondence analysis of bio-refractory compounds degradation and microbiological community distribution in anaerobic filter for coking wastewater treatment. *Chemical Engineering Journal* **304**, 864-872 (2016)10.1016/j.cej.2016.05.142).
6. D. C. Kalyani, P. S. Patil, J. P. Jadhav, S. P. Govindwar, Biodegradation of reactive textile dye Red BLI by an isolated bacterium Pseudomonas sp. SUK1. *Bioresource technology* **99**, 4635-4641 (2008); published online EpubJul (10.1016/j.biortech.2007.06.058).
7. E. Z. Wang, Y. Wang, D. Xiao, Polymer Nanocomposites for Photocatalytic Degradation and Photoinduced Utilizations of Azo-Dyes. *Polymers* **13**, 1215 (2021).
8. G. Rajhans, S. K. Sen, A. Barik, S. Raut, Elucidation of fungal dye-decolourizing peroxidase (DyP) and ligninolytic enzyme activities in decolourization and mineralization of azo dyes. *Journal of applied microbiology* **129**, 1633-1643 (2020); published online EpubDec (10.1111/jam.14731).
9. C. Zhang, H. Chen, G. Xue, Y. Liu, S. Chen, C. Jia, A critical review of the aniline transformation fate in azo dye wastewater treatment. *Journal of Cleaner Production* **321**, 128971 (2021)10.1016/j.jclepro.2021.128971).
10. M. Esterhuizen, S. Behnam Sani, L. Wang, Y. J. Kim, S. Pflugmacher, Mycoremediation of acetaminophen: Culture parameter optimization to improve efficacy.

Chemosphere **263**, 128117 (2021)10.1016/j.chemosphere.2020.128117).

11. N. Akhtar, M. A.-u. Mannan, Mycoremediation: Expunging environmental pollutants. *Biotechnology Reports* **26**, e00452 (2020)10.1016/j.btre.2020.e00452).

12. A. M. Q. López, A. L. d. S. Silva, E. C. L. d. Santos, The fungal ability for biobleaching/biopulping/bioremediation of lignin-like compounds of agro-industrial raw material. *Química Nova* **40**, 916-931 (2017).

13. F. J. Márquez-Rocha, V. Z. Hernández-Rodríguez, R. Vázquez-Duhalt, Biodegradation of soil-adsorbed polycyclic aromatic hydrocarbons by the white rot fungus Pleurotus ostreatus. *Biotechnology letters* **22**, 469-472 (2000).

14. A. Khalid, M. Arshad, D. Crowley, Bioaugmentation of azo dyes. *Biodegradation of Azo Dyes*, 1-37 (2010).

15. G. Pathiraja, P. Egodawatta, A. Goonetilleke, V. S. J. Te'o, Solubilization and degradation of polychlorinated biphenyls (PCBs) by naturally occurring facultative anaerobic bacteria. *Science of The Total Environment* **651**, 2197-2207 (2019)10.1016/j.scitotenv.2018.10.127).

16. Z. Chen, Y. Jiang, Z. Chang, J. Wang, X. Song, Z. Huang, S. Chen, J. Li, Denitrification characteristics and pathways of a facultative anaerobic denitrifying strain, Pseudomonas denitrificans G1. *Journal of bioscience and bioengineering* **129**, 715-722 (2020)10.1016/j.jbiosc.2019.12.011).

17. A. Jain, J. A. Gralnick, Evidence for auxiliary anaerobic metabolism in obligately aerobic Zetaproteobacteria. *The ISME journal* **14**, 1057-1062 (2020); published online EpubApr (10.1038/s41396-020-0586-6).

18. R. E. Bradshaw, D. M. Bird, S. Brown, R. E. Gardiner, P. Hirst, Cytochrome c is not essential for viability of the fungus Aspergillus nidulans. *Molecular genetics and genomics : MGG* **266**, 48-55 (2001); published online EpubSep (10.1007/s004380100517).

19. R. A. Lockington, G. N. Borlace, J. M. Kelly, Pyruvate decarboxylase and anaerobic survival in Aspergillus nidulans. *Gene* **191**, 61-67 (1997); published online EpubMay 20 (10.1016/s0378-1119(97)00032-2).

20. P. A. Belinky, N. Flikshtein, S. Lechenko, S. Gepstein, C. G. Dosoretz, Reactive oxygen species and induction of lignin peroxidase in Phanerochaete chrysosporium. *Applied and environmental microbiology* **69**, 6500-6506 (2003); published online EpubNov (10.1128/aem.69.11.6500-6506.2003).

21. V. Matikka, H. Heinonen-Tanski, Reduction of phosphorus, nitrogen and microorganisms in pilot scale sand filter beds containing biotite, treating primary wastewater. *Environmental technology* **37**, 46-54 (2016)10.1080/09593330.2015.1063703).

22. S. Kleindienst, K. Chourey, G. Chen, R. W. Murdoch, S. A. Higgins, R. Iyer, S. R. Campagna, E. E. Mack, E. S. Seger, R. L. Hettich, Proteogenomics reveals novel reductive dehalogenases and methyltransferases expressed during anaerobic dichloromethane metabolism. *Applied and environmental microbiology* **85**, e02768-02718 (2019).

23. C. Liu, L. Ren, B. Yan, L. Luo, J. Zhang, M. K. Awasthi, Electron transfer and mechanism of energy production among syntrophic bacteria during acidogenic fermentation: A review. *Bioresource technology* **323**, 124637 (2021); published online Epub2021/03/01/ (https://doi.org/10.1016/j.biortech.2020.124637).

24. H. Han, Y. Zheng, T. Zhou, P. Liu, X. Li, Cu(II) nonspecifically binding chromate

reductase NfoR promotes Cr(VI) reduction. *Environmental microbiology* **23**, 415-430 (2020)10.1111/1462-2920.15329).

25. C. He, Y. Huang, P. Liu, J. Wei, Y. Yang, L. Xu, M. Xiao, Transcriptome analysis of genes and metabolic pathways associated with nicotine degradation in Aspergillus oryzae 112822. *BMC genomics* **20**, 86 (2019); published online EpubJan 24 (10.1186/s12864-019-5446-2).

26. S. K. Das, I. Shome, A. K. Guha, Surface functionalization of Aspergillus versicolor mycelia: in situ fabrication of cadmium sulphide nanoparticles and removal of cadmium ions from aqueous solution. *RSC advances* **2**, 3000 (2012)10.1039/c2ra01273a).

27. G. K. Villena, T. Fujikawa, S. Tsuyumu, M. Gutiérrez-Correa, Structural analysis of biofilms and pellets of Aspergillus niger by confocal laser scanning microscopy and cryo scanning electron microscopy. *Bioresource technology* **101**, 1920-1926 (2010)10.1016/j.biortech.2009.10.036).

28. Q. Li, X. L. Feng, T. T. Li, X. R. Lu, Q. Y. Liu, X. Han, Y. J. Feng, Z. Y. Liu, X. J. Zhang, X. Xiao, Anaerobic decolorization and detoxification of cationic red X-GRL by Shewanella oneidensis MR-1. *Environmental technology* **39**, 2382-2389 (2018); published online EpubSep (10.1080/09593330.2017.1355933).

29. S. Renganathan, W. R. Thilagaraj, L. R. Miranda, P. Gautam, M. Velan, Accumulation of Acid Orange 7, Acid Red 18 and Reactive Black 5 by growing Schizophyllum commune. *Bioresource technology* **97**, 2189-2193 (2006)10.1016/j.biortech.2005.09.018).

30. Y. Yang, D. Jin, G. Wang, S. Wang, X. Jia, Y. Zhao, Competitive biosorption of Acid Blue 25 and Acid Red 337 onto unmodified and CDAB-modified biomass of Aspergillus oryzae. *Bioresource technology* **102**, 7429-7436 (2011); published online Epub2011/08/01/ (https://doi.org/10.1016/j.biortech.2011.05.023).

31. L. Kumari, D. Tiwary, P. K. Mishra, Biodegradation of C.I. Acid Red 1 by indigenous bacteria Stenotrophomonas sp. BHUSSp X2 isolated from dye contaminated soil. *Environmental Science and Pollution Research* **23**, 4054-4062 (2015)10.1007/s11356-015-4351-8).

32. S. R. Dave, R. H. Dave, Isolation and characterization of Bacillus thuringiensis for Acid red 119 dye decolourisation. *Bioresource technology* **100**, 249-253 (2009)10.1016/j.biortech.2008.05.019).

33. A. Stolz, Basic and applied aspects in the microbial degradation of azo dyes. *Applied microbiology and biotechnology* **56**, 69-80 (2001)10.1007/s002530100686).

34. R. U. Meckenstock, M. Boll, H. Mouttaki, J. S. Koelschbach, P. Cunha Tarouco, P. Weyrauch, X. Dong, A. M. Himmelberg, Anaerobic Degradation of Benzene and Polycyclic Aromatic Hydrocarbons. *Microbial Physiology* **26**, 92-118 (2016)10.1159/000441358).

35. R. Martens, F. Zadrazil, Screening of white-rot fungi for their ability to mineralize polycyclic aromatic hydrocarbons in soil. *Folia microbiologica* **43**, 97-103 (1998)10.1007/bf02815552).

36. T. F. Guerin, Ex-situ bioremediation of chlorobenzenes in soil. *Journal of hazardous materials* **154**, 9-20 (2008); published online EpubJun 15 (10.1016/j.jhazmat.2007.09.094).

37. F. Révész, M. Farkas, B. Kriszt, S. Szoboszlay, T. Benedek, A. Táncsics, Effect of

608 oxygen limitation on the enrichment of bacteria degrading either benzene or toluene and the
609 identification of Malikia spinosa (Comamonadaceae) as prominent aerobic benzene-, toluene-,
610 and ethylbenzene-degrading bacterium: enrichment, isolation and whole-genome analysis.
611 *Environmental Science and Pollution Research* **27**, 31130-31142
612 (2020)10.1007/s11356-020-09277-z).
613 38. T. Hiromoto, S. Fujiwara, K. Hosokawa, H. Yamaguchi, Crystal structure of
614 3-hydroxybenzoate hydroxylase from Comamonas testosteroni has a large tunnel for substrate
615 and oxygen access to the active site. *Journal of molecular biology* **364**, 878-896 (2006);
616 published online EpubDec 15 (10.1016/j.jmb.2006.09.031).
617 39. H. Yu, S. Zhao, W. Lu, W. Wang, L. Guo, A novel gene, encoding
618 3-aminobenzoate 6-monooxygenase, involved in 3-aminobenzoate degradation in Comamonas
619 sp. strain QT12. *Applied microbiology and biotechnology* **102**, 4843-4852 (2018); published
620 online EpubJun (10.1007/s00253-018-9015-4).
621 40. B. G. Hall, L. Xu, Nucleotide sequence, function, activation, and evolution of the
622 cryptic asc operon of Escherichia coli K12. *Molecular biology and evolution* **9**, 688-706
623 (1992); published online EpubJul (10.1093/oxfordjournals.molbev.a040753).
624 41. D. S. Frear, Herbicide metabolism in plants—I: Purification and properties of
625 UDP-glucose: Arylamine N-glucosyl-transferase from soybean. *Phytochemistry* **7**, 381-390
626 (1968); published online Epub1968/03/01/ (https://doi.org/10.1016/S0031-9422(00)90876-8).
627 42. Z. Dai, Y. Zhu, H. Dong, C. Zhao, Y. Zhang, Y. Li, Enforcing ATP hydrolysis
628 enhanced anaerobic glycolysis and promoted solvent production in Clostridium
629 acetobutylicum. *Microbial Cell Factories* **20**, (2021)10.1186/s12934-021-01639-7).
630 43. X. Yu, Y. Jiang, H. Huang, J. Shi, K. Wu, P. Zhang, J. Lv, H. Li, H. He, P. Liu, X.
631 Li, Simultaneous aerobic denitrification and Cr(VI) reduction by Pseudomonas
632 brassicacearum LZ-4 in wastewater. *Bioresource technology* **221**, 121-129 (2016); published
633 online EpubDec (10.1016/j.biortech.2016.09.037).
634 44. K. V. Solomon, C. H. Haitjema, J. K. Henske, S. P. Gilmore, D. Borges-Rivera, A.
635 Lipzen, H. M. Brewer, S. O. Purvine, A. T. Wright, M. K. Theodorou, I. V. Grigoriev, A.
636 Regev, D. A. Thompson, M. A. O'Malley, Early-branching gut fungi possess a large,
637 comprehensive array of biomass-degrading enzymes. *Science* **351**, 1192-1195 (2016);
638 published online EpubMar 11 (10.1126/science.aad1431).
639 45. A. Oakley, Glutathione transferases: a structural perspective. *Drug metabolism*
640 *reviews* **43**, 138-151 (2011).
641 46. J. Baier, M. Gänsbauer, C. Giessler, H. Arnold, M. Muske, U. Schleicher, S.
642 Lukassen, A. Ekici, M. Rauh, C. Daniel, A. H. rtmann, B. Schmid, P. Tripal, K. Dettmer, P. J.
643 Oefner, R. Atreya, S. Wirtz, C. Bogdan, J. Mattner, Arginase impedes the resolution of colitis
644 by altering the microbiome and metabolome. *Journal of Clinical Investigation* **130**, 5703-5720
645 (2020)10.1172/jci126923).
646 47. H. S. Park, S. C. Jun, K. H. Han, S. B. Hong, J. H. Yu, Diversity, Application, and
647 Synthetic Biology of Industrially Important Aspergillus Fungi. *Advances in applied*
648 *microbiology* **100**, 161-202 (2017)10.1016/bs.aambs.2017.03.001).
649 48. V. Arantes, A. M. Milagres, T. R. Filley, B. Goodell, Lignocellulosic
650 polysaccharides and lignin degradation by wood decay fungi: the relevance of nonenzymatic
651 Fenton-based reactions. *Journal of industrial microbiology & biotechnology* **38**, 541-555

652 (2011); published online EpubApr (10.1007/s10295-010-0798-2).

653

654

655 **Figure captions**

656

657 Fig. 1 The identification of fungi LZ-M and its decolorization of acid red 73
658 under anaerobic condition. (A) Phylogenetic tree of strain LZ-M based on ITS
659 sequencing; (B) Anaerobic decolorization process of fungi LZ-M mycelium in
660 anaerobic tubes; (C) Scanning electron microscope images of the surface structure of
661 mycelium: (i) mycelium after aerobic culture for 48h; (ii) mycelium at initial time of
662 anaerobic culture; (iii) mycelium after anaerobic culture for 24h; (iv) mycelium after
663 anaerobic culture for 48 h.

664 Fig. 2 Effect factors of anaerobic decolorization of AR73 by *A. tabacinus* LZ-M
665 and its degradation ability on other organic matter. (A) Variation curve of AR73 under
666 aerobic and anaerobic conditions at different time; The effect of different carbon
667 sources (B), AR73 concentrations (C) and pH (D) on decolorization; (E) Continuous
668 decolorization of AR73 with multiple addition; (F) Anaerobic degradation of *A.*
669 *tabacinus* LZ-M on different organic matters. All reaction experiments were

670 Fig. 3 The degradation pathway of AR73 by *A. tabacinus* LZ-M. (A)
671 Presumptive metabolic pathway of AR73 based on the products in LC-MS analysis
672 results; The contents of phenylhydrazine (B), aniline (C) and CO_2 (D) in anaerobic
673 culture at differe

674 Fig. 4 Expression counts of gene in *A. tabacinus* LZ-M after anaerobic and
675 aerobic culture by transcriptome sequencing, including glycolysis process, aromatics
676 degradation, cytochrome C oxidase and quinone oxidoreductase related genes.

677 Fig. 5 Unknown gene expression and function identification. (A) The distribution
678 of oxidoreductase genes and unknown genes among the top 140 genes of up-regulated
679 expression (count value > 150, up-regulated multiple > 4); (B) The unknown genes such
680 as Ord95 and Ord118 after expression and purification were showed in the SDS-PAGE;
681 (C, D) Dehydrogenase activity assay of Ord118 and Ord95 (mean ± SE, n = 3); (E-F)
682 AR73 decolorization activity analysis of Ord95 (mean ± SE, n = 3). The concentrations
683 of enzyme used were 0.28 mg/L.

684 Fig. 6 Products of enzymatic degradation of AR73 and structural prediction of
685 Ord95 protein. (A) Determination of aniline and phenylhydrazine in AR73 enzymatic
686 reaction solution by HPLC; (B) Changes of aniline and phenylhydrazine concentrations
687 in AR73 enzymatic reaction solution with time (mean ± SE, n = 3); (C) SDS-PAGE
688 image of Ord95 point mutant protein; (D) Relative enzyme activity of Ord95 point
689 mutant protein (mean ± SE, n = 3); (E, F) Model constructions of Ord95 protein with
690 SWISS-MODEL. The green dots are 38R, 54R, 55R mutation sites.

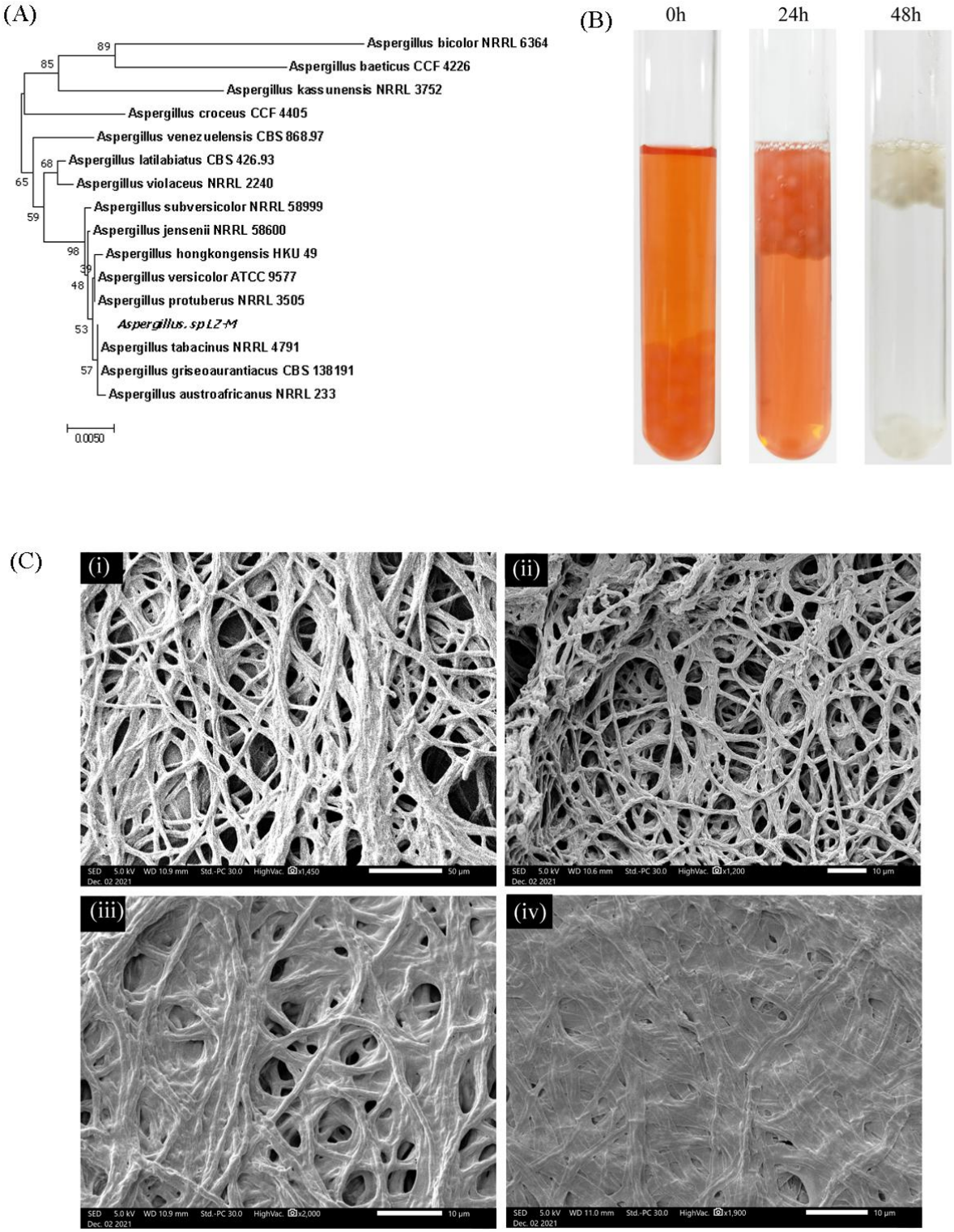

Fig. 1

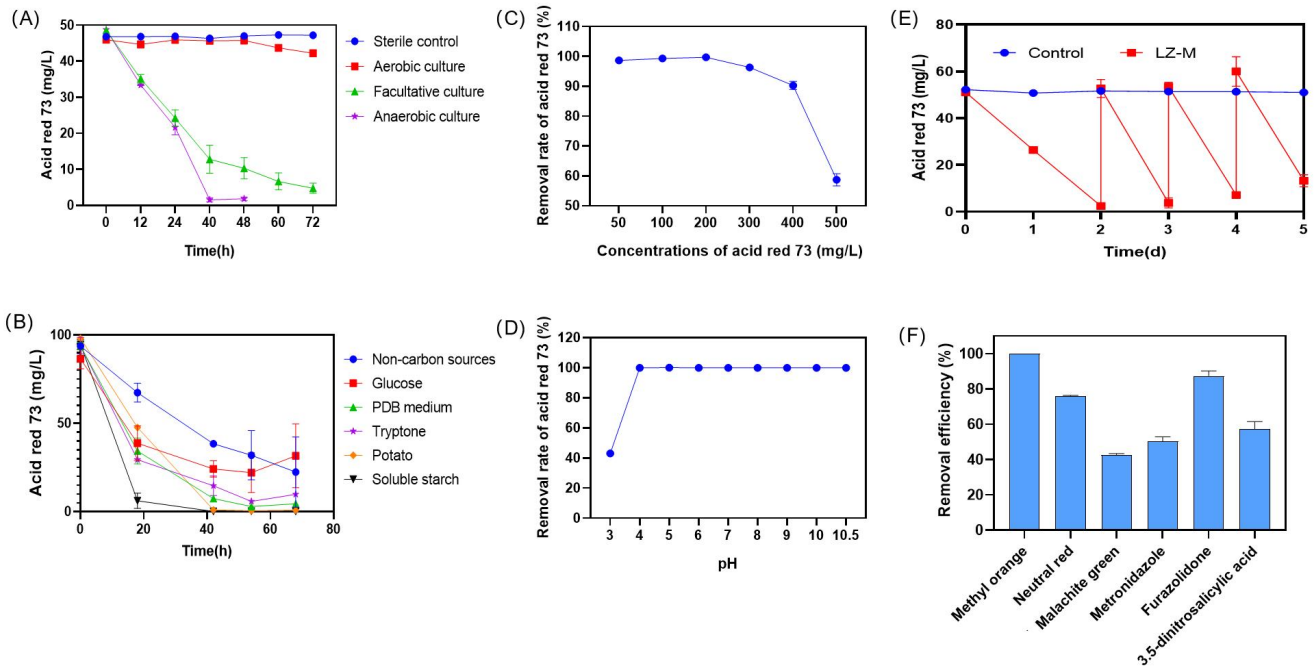

Fig. 2

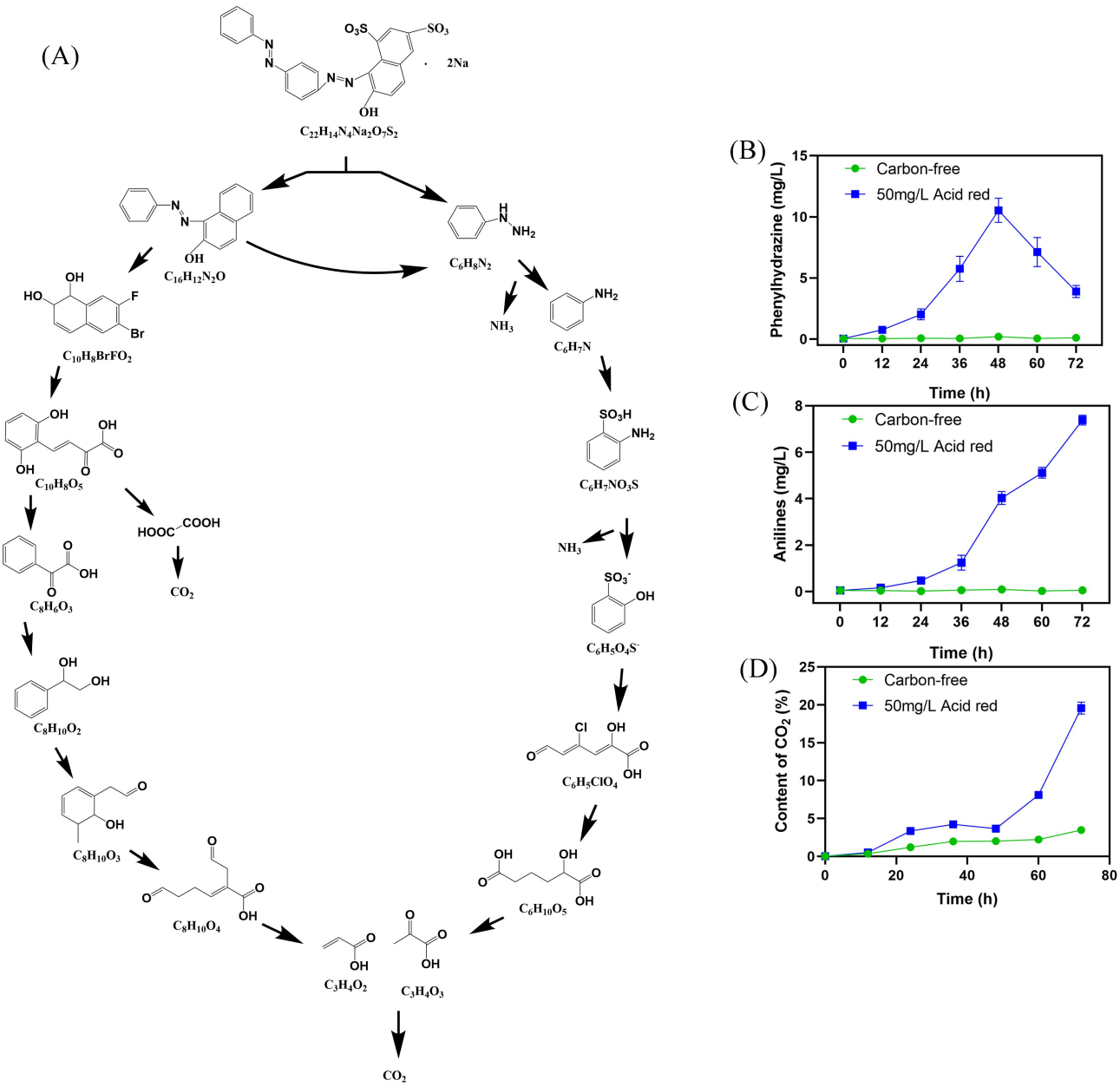

Fig. 3

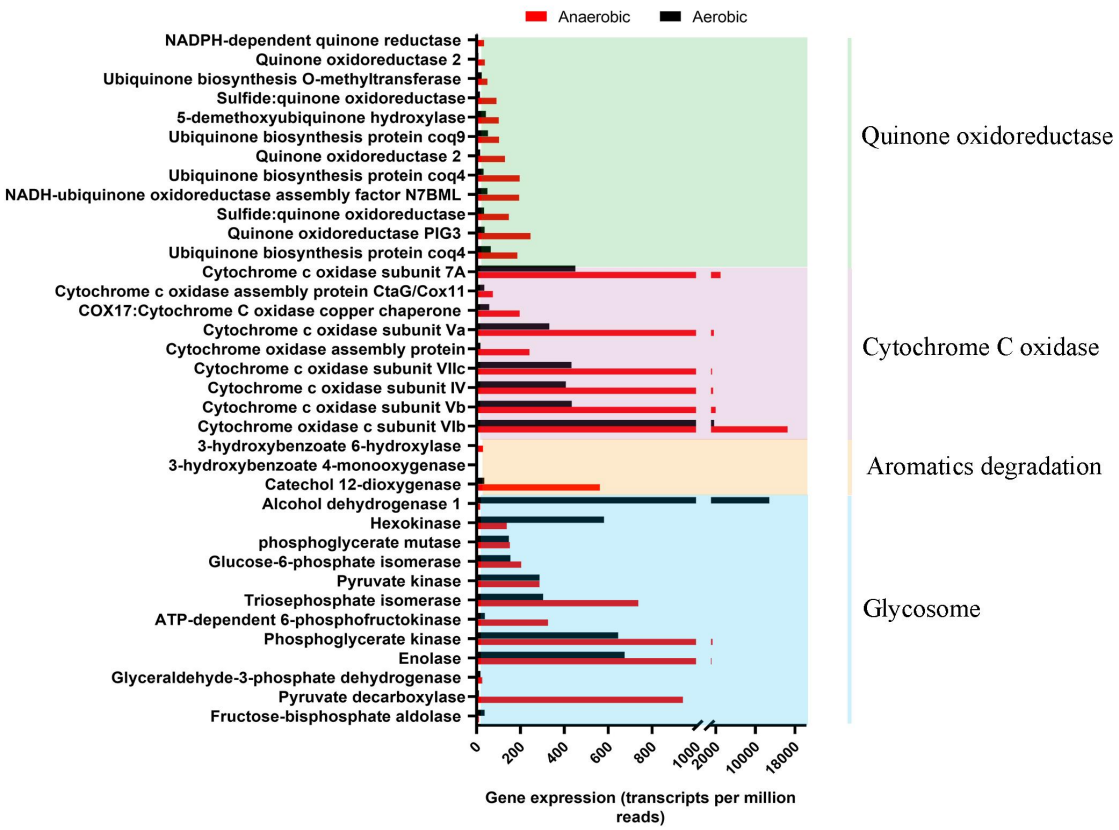

Fig. 4

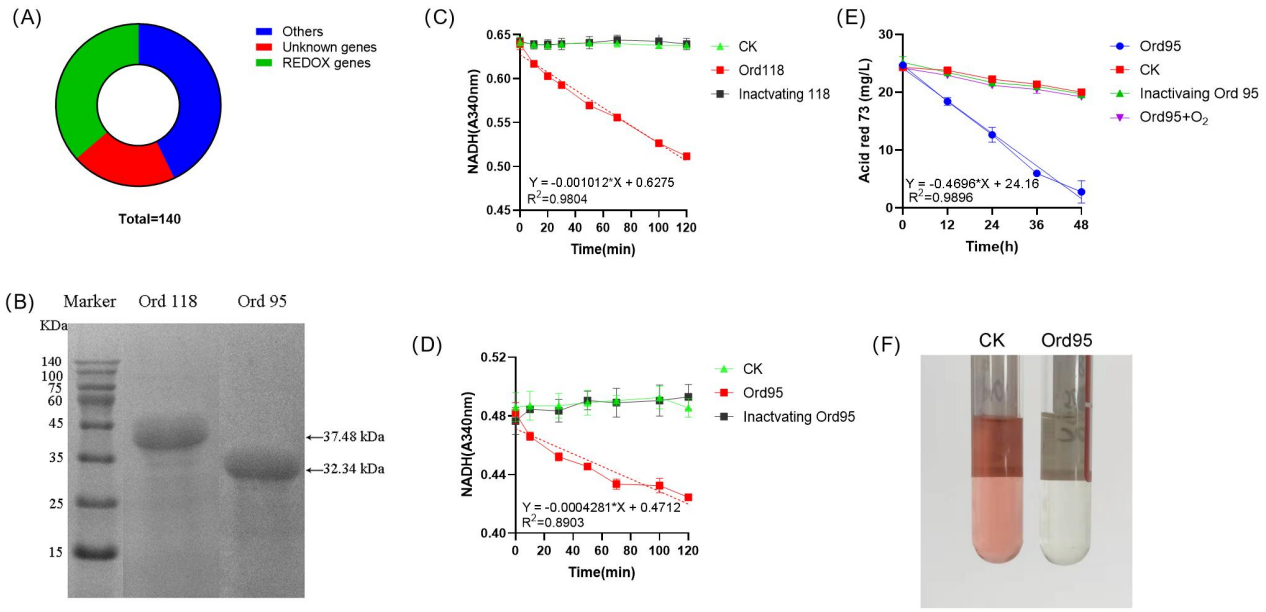

Fig. 5

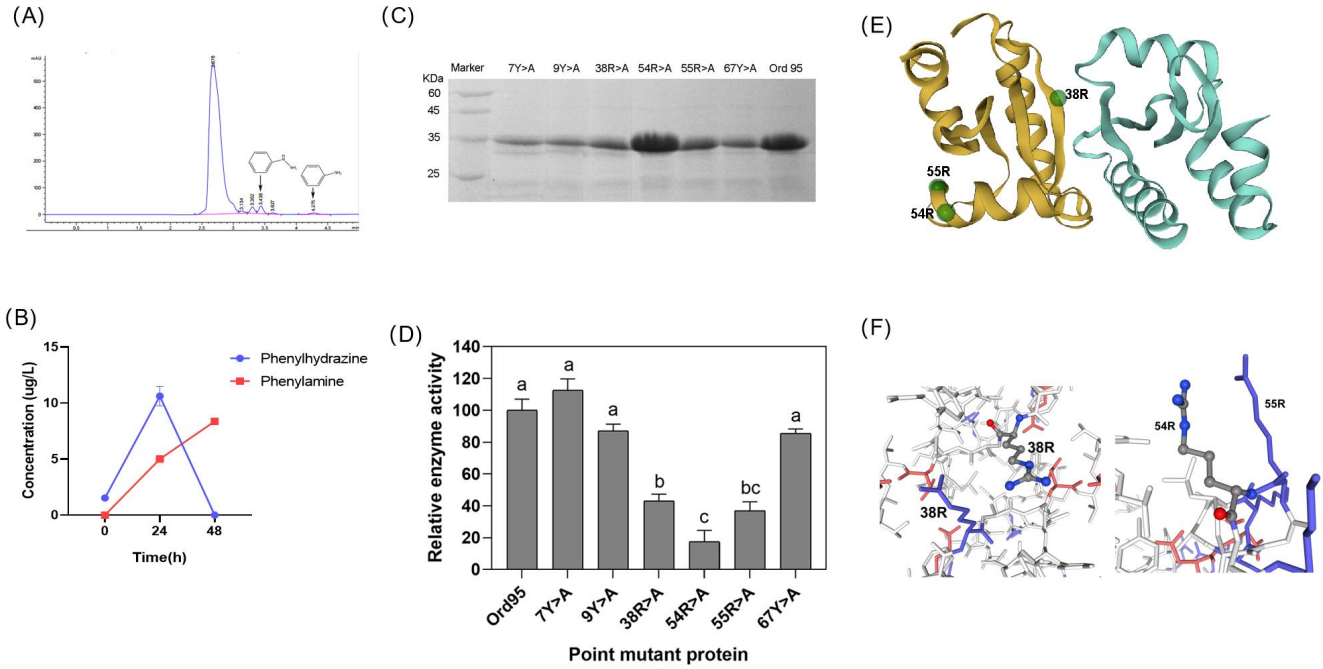

Fig. 6